AFRL-AFOSR-VA-TR-2022-0382

Knowledge-Driven Design and Optimization of New Types of Yarn and Fiber Artificial Muscles

Baughman, Ray
UNIVERSITY OF TEXAS AT DALLAS
800 W CAMPBELL RD
RICHARDSON, TX, 75080
USA

07/14/2022
Final Technical Report

Air Force Research Laboratory
Air Force Office of Scientific Research
Arlington, Virginia 22203
Air Force Materiel Command

REPORT DOCUMENTATION PAGE

PLEASE DO NOT RETURN YOUR FORM TO THE ABOVE ORGANIZATION.

1. REPORT DATE	2. REPORT TYPE	3. DATES COVERED	
20220714	Final	START DATE 20180815	END DATE 20210814

4. TITLE AND SUBTITLE
Knowledge-Driven Design and Optimization of New Types of Yarn and Fiber Artificial Muscles

5a. CONTRACT NUMBER	5b. GRANT NUMBER	5c. PROGRAM ELEMENT NUMBER
	FA9550-18-1-0510	61102F
5d. PROJECT NUMBER	**5e. TASK NUMBER**	**5f. WORK UNIT NUMBER**

6. AUTHOR(S)
Ray Baughman

7. PERFORMING ORGANIZATION NAME(S) AND ADDRESS(ES)
UNIVERSITY OF TEXAS AT DALLAS
800 W CAMPBELL RD
RICHARDSON, TX 75080
USA

8. PERFORMING ORGANIZATION REPORT NUMBER

9. SPONSORING/MONITORING AGENCY NAME(S) AND ADDRESS(ES)	10. SPONSOR/MONITOR'S ACRONYM(S)	11. SPONSOR/MONITOR'S REPORT NUMBER(S)
Air Force Office of Scientific Research 875 N. Randolph St. Room 3112 Arlington, VA 22203	AFRL/AFOSR RTB2	AFRL-AFOSR-VA-TR-2022-0382

12. DISTRIBUTION/AVAILABILITY STATEMENT
A Distribution Unlimited: PB Public Release

13. SUPPLEMENTARY NOTES

14. ABSTRACT
This 3rd year and final report mainly summarizes our project-supported 2021 publication in Science ( ) on unipolar-stroke, electroosmotic-pump carbon nanotube yarn muscles. Previous electrochemical carbon nanotube yarn muscles cannot be usefully operated between the extreme potentials of the electrochemical stability window, since the muscle's stroke during electron and hole injection partially cancel. In contrast, the stroke changes of our unipolar stroke carbon nanotube yarn between extreme potentials are additive and in important cases muscle stroke remarkably increases with increasing potential scan rate. The normal decrease in stroke with increasing scan rate, because of decreased capacitance, is overwhelmed by a dramatic increase in effective ion size caused by electroosmotic pumping of solvent. These coiled carbon nanotube yarn muscles contain a yarn guest that shifts the yarn's potential of zero charge by over a volt, either positively or negatively. Such pzc shift agents include ion-exchange membrane polymers, oxidized graphene platelets, and surfactants. Record muscle strokes, contractile work-per-cycle, contractile power densities, and energy conversion efficiencies are obtained for unipolar muscles having scan-rate enhanced stroke, and theory is used to understand results. Other key breakthroughs made this project year cannot be disclosed in this publicly available report because of ongoing patent filings, but will be fully described in following reports. Three US patent issuances, three US patent allowances, and 2 US patent filings have been made in the project year for AFOSR sponsored work. Also, one of our patent licensees has used our thermally powered muscles to manufacture comfort adjusting jackets that exploit environmental temperature changes to power changes in jacket insulation.

15. SUBJECT TERMS

16. SECURITY CLASSIFICATION OF:			17. LIMITATION OF ABSTRACT	18. NUMBER OF PAGES
a. REPORT	b. ABSTRACT	c. THIS PAGE		
U	U	U	UU	13

19a. NAME OF RESPONSIBLE PERSON	19b. PHONE NUMBER *(Include area code)*
BYUNG LEE	426-8483

Final Year Report for FA9550-18-1-0510 on "Knowledge-Driven Design and Optimization of New Types of Yarn and Fiber Artificial Muscles"

Period: 8/20/2020 - 8/19/2021

Abstract

This 3rd year and final report mainly summarizes our project-supported 2021 publication in Science (*1*) on unipolar-stroke, electroosmotic-pump carbon nanotube yarn muscles. Previous electrochemical carbon nanotube yarn muscles cannot be usefully operated between the extreme potentials of the electrochemical stability window, since the muscle's stroke during electron and hole injection partially cancel. In contrast, the stroke changes of our unipolar stroke carbon nanotube yarn between extreme potentials are additive and in important cases muscle stroke remarkably increases with increasing potential scan rate. The normal decrease in stroke with increasing scan rate, because of decreased capacitance, is overwhelmed by a dramatic increase in effective ion size caused by electroosmotic pumping of solvent. These coiled carbon nanotube yarn muscles contain a yarn guest that shifts the yarn's potential of zero charge by over a volt, either positively or negatively. Such pzc shift agents include ion-exchange membrane polymers, oxidized graphene platelets, and surfactants. Record muscle strokes, contractile work-per-cycle, contractile power densities, and energy conversion efficiencies are obtained for unipolar muscles having scan-rate enhanced stroke, and theory is used to understand results. Other key breakthroughs made this project year cannot be disclosed in this publicly available report because of ongoing patent filings, but will be fully described in following reports. Three US patent issuances, three US patent allowances, and 2 US patent filings have been made in the project year for AFOSR sponsored work. Also, one of our patent licensees has used our thermally powered muscles to manufacture comfort adjusting jackets that exploit environmental temperature changes to power changes in jacket insulation.

1. Project results for unipolar-stroke, electroosmotic-pump carbon nanotube yarn muscles

Introduction

We here focus on electrochemical driven coiled yarn muscles, because of their higher energy conversion efficiency than thermal muscles and their ability to maintain stroke without consuming much energy. Electrochemical double-layer charge injection forces neighboring CNTs or CNT bundles apart, which increases yarn diameter and causes muscle length contraction. This contraction can be understood for a twisted non-coiled muscle that is torsionally tethered (like the presently described muscles), since an increase in yarn diameter increases the path length per yarn length of the helically configured CNTs that result from twist insertion. Coiling amplifies muscle stroke by using changes of yarn twist (resulting from conversion between the twist of coiling and yarn twist) to drive changes in muscle length.

We here provide solutions to a major problem that exists for present electrochemical CNT artificial muscles. During a scan from extreme negative to extreme positive potentials, there is first an efflux of positive ions and then an influx of negative ions for the electrochemical double layer. Hence, these muscles are bipolar, meaning that they both expand and contract during a scan from extreme negative to extreme positive potentials, so the net effect is a decrease in overall stroke. Contrastingly, the stroke of a unipolar artificial muscle monotonically changes during a potential scan over the entire electrochemical window. We demonstrated record performance for unipolar muscles that utilize the enabled extreme potentials, especially those providing the strange property

of increasing stroke with increasing potential scan rate, which we call scan rate enhanced stroke (SRES).

Unipolar tensile actuation is observed for Faradaic electrochemical muscles in which only one sign ion participates in an intercalation-based process over the available potential range. However, Faradaic intercalation generally suffers from rate and cyclability limitations, as seen by comparing battery and supercapacitor performance. While unipolar electrochemical double-layer actuation has been observed for other systems (at least in the reported potential range), the combination of unipolar actuation with SRES has not been reported for a high-performance muscle, and this combination results in the presently described remarkable muscle performance. Although the ability to shift the potential of zero charge to outside the electrochemical window is key for the present work, it has not been previously discussed as a means for increasing muscle performance.

The reported work capacities and power densities are for muscle contraction. For an optimized step-potential change, the full-cycle power density is the contractile work-per-cycle divided by the cycle time and the maximum average power density is the ratio of contractile work to actuation time for an optimized time. The reference electrodes in aqueous and organic electrolytes were Ag/AgCl and platinum, respectively, and all potentials are relative to these references. Unless otherwise noted, tensile actuation was characterized under constant load, while the yarn was torsionally tethered, a large capacitance counter electrode was used, current densities are relative to the weight of the dry muscle, and capacitances and injected charge are relative to the weight of CNTs. For fairly comparing, unipolar and bipolar actuation, the performance metrics of bipolar muscles includes only potential ranges where stroke cancellation does not occur.

Unipolar CNT muscles with SRES using ion-exchange membrane polymers as yarn guest

The previous record for contractile work capacity (the work during muscle contraction) of an electrochemical CNT muscle in an aqueous electrolyte was our 0.24 J/g, which was for a coiled CNT yarn containing reduced graphene oxide (*2*). In the present work, we demonstrated that this work capacity in an aqueous electrolyte can be increased to 1.04 J/g by transitioning from a bipolar muscle to a unipolar CNT yarn muscle in which the CNT are coated with an ion-exchange membrane polymer (i.e, an ionomer). The first investigated polymer was poly(sodium 4-styrenesulfonate) (PSS), which is approved for drug use and cheap enough for use in water softening. A PSS guest in a CNT yarn is called a PSS@CNT yarn. When the host ionomer had initially a different mobile anion (or cation) than for the electrolyte in the surrounding liquid electrolyte, the muscle was electrochemically cycled until fully reversible actuation resulted, implying that the original ion in the ionomer was replaced by the ion in the liquid electrolyte.

A typically used muscle fabrication method is shown in Fig. 1A. Approximately 5 highly aligned, 5-cm-wide CNT sheets were draw from a carbon multiwall nanotube (MWNT) forest and stacked together, infiltrated with polymer by deposition from an aqueous solution, and then the sheet stack was twisted until fully coiled. Unless otherwise described for neat and guest-containing muscles, the twisted yarn's diameter before the onset of coiling was 80 to 120 μm, and the applied load during twist insertion was 10 to 20 MPa (when normalized to the yarn's cross-sectional area before the onset of coiling). Transmission electron microscope images of the cross-section of a coiled 40 wt % PSS@CNT muscle show that the PSS strongly binds to the surfaces of CNT bundles. Unipolar and bipolar actuation are schematically illustrated in Fig. 1B.

The dependence of measured contractile strokes on the applied potential are shown in Figs. 2A and B for a bipolar neat yarn and a unipolar PSS@CNT yarn, respectively, in 0.1 M aqueous LiCl electrolyte. About 30 wt % PSS was used to optimize performance. Piezoelectrochemical

spectroscopy (PECS) indicates the origin of this transition from bipolar to unipolar actuation. When using our PECS method (*3*), a cyclic voltammetry (CV) scan is conducted while the yarn is sinusoidally stretched. The potential of zero charge (pzc) is the potential at which the stretch-induced current change becomes zero. The PECS results (Figs. 2C and D) show that the bipolar behavior of the neat yarn converts to the unipolar behavior of the 30 wt % PSS@CNT yarn because of a polymer-induced shift of the pzc from -80 mV to above +1 V, which is outside the electrochemical stability window of the electrolyte. The PECS measurements show that the shift of the pzc monotonically increases with increasing PSS concentration, and that this shift is independent of the pH of the electrolyte (and the resulting charge transfer) for a coiled CNT yarn.

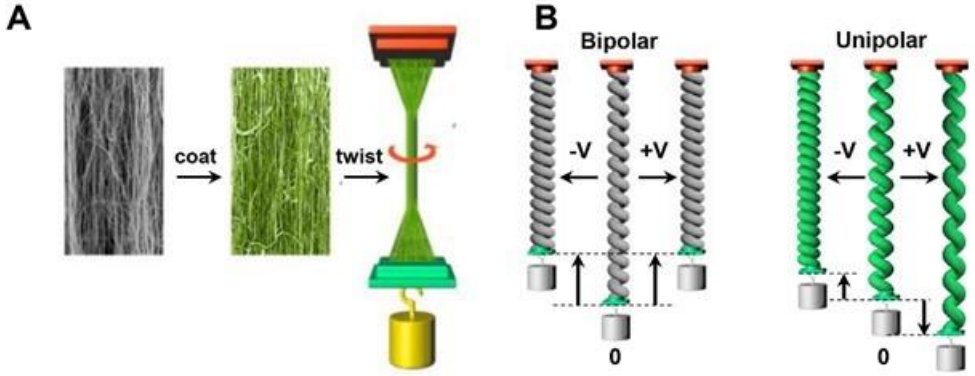

Fig. 1. Fabrication of a unipolar muscle and comparison of actuation with a bipolar muscle. (**A**) Illustration of the fabrication of a unipolar muscle by infiltrating a neat CNT sheet (left) with an ionomer (middle), and inserting twist into this sheet to produce coiling of the CNT yarn (right). (**B**) Schematic illustration of the difference between bipolar and unipolar stroke muscle actuation.

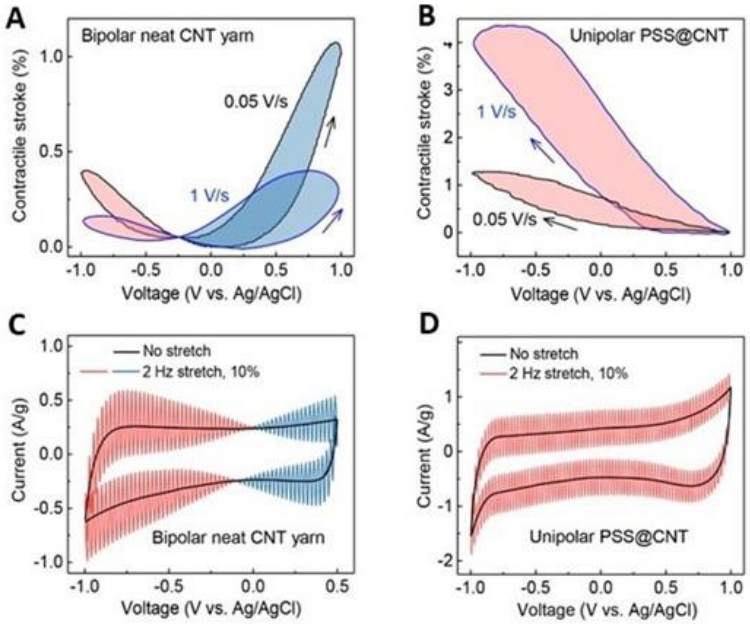

Fig. 2. Comparison of actuation for unipolar muscle and bipolar muscles. (**A**, **B**) Tensile stroke under 10.9 MPa load for different cyclic voltammetry scan rates for a neat CNT yarn muscle and a PSS@CNT yarn muscle, respectively, in 0.1 M aqueous LiCl. (**C**, **D**) Piezoelectrochemical spectroscopy for a scan rate of 50 mV/s for a neat CNT yarn muscle and a PSS@CNT yarn muscle, respectively, in the above electrolyte. A sinusoidal tensile strain of 10% at 2 Hz was applied. The potential at which the stretch-induced current change vanishes indicates that the pzc of the neat CNT yarn is -80 mV, and that the pzc of the unipolar PSS@CNT yarn is outside the electrochemical window of the aqueous electrolyte.

While previous electrochemical yarn muscles decrease stroke with increasing potential scan rate, the stroke of this unipolar muscle containing 30 wt % PSS (Fig. 3A) dramatically increases (by a factor of 3.8 for a scan rate increase from 0.01 V/s to 1 V/s, which is called the SRES enhancement). In order to quantify the effects of this SRES on effective ion size (Fig. 3B), the scan-rate dependence of the stroke-charge ratio (SCR) was measured, which is the ratio of muscle stroke to the change in gravimetric charge per CNT weight for a given potential scan range. These results show that the SCR of the neat CNT yarn is very low for both electron and hole injection, and even slightly decreases in magnitude with increasing potential scan rate. However, the SCR for the PSS@CNT yarns dramatically increase with increasing scan rate (Fig. 3B). This result shows that the effective ion size increases with increasing potential scan rate, which is caused by electroosmotic pumping of solvent. This effective ion size includes the ion hydration observed at low scan rates, as well as the water that is dragged by the hydrated ion at high scan rates. We observed that the coulombic efficiency is sufficiently high for these experiments that charge loss does not significantly affect the stroke-charge ratio.

These results are like those for well-known water transport through membranes, which has been used for pumping water between reservoirs. Analogous water pumping has been observed for ionic polymer-metal composite (IPMC) bending actuators. Upon increasing the charge transfer rate, the hydrated ion drags additional water. The SRES enhancement for a 0.1 M aqueous salt concentration is much lower for NaCl electrolyte (2.7) than for the LiCl aqueous electrolyte (3.8). This is likely due to the higher negative hydration enthalpy of Li^+, which allows a stronger interaction with surrounding water dipoles and leads to an increased water transference coefficient.

Further evidence for a scan rate dependence of effective ion size was obtained from electrochemical quartz crystal microbalance measurements of the scan rate dependence of weight increase per injected charge for a CNT sheet stack containing 40 wt % PSS. The transported water increased monotonically from 5.2 to 7.1 H_2O/Li^+ with increasing potential scan rate from 10 mV/s to 100 mV/s for the PSS@CNT sheet stack, while it was approximately constant over this scan rate range (between 5.9 to 5.5 H_2O/Li^+) for a neat CNT sheet stack. Weight change measurements during CV scans show unipolar weight pickup for the 40 wt % PSS@CNT sheet stack and bipolar weight pickup for the neat CNT sheet stack.

The dramatic effect of SRES can also be seen for actuation of a 30 wt % PSS@CNT muscle in a 0.1 M aqueous LiCl electrolyte, when using the large amplitude square wave potentials that are enabled by unipolar behavior. The small stroke observed for the neat CNT yarn (Fig. 3C) rapidly decreases with increasing frequency, since no effect is available to compensate for the decrease of capacitance with increasing frequency. In contrast, the existence of SRES means that a large increase in effective ion size results for the high charge injection rates obtained for square wave potentials, which partially compensates for this capacitance decrease. The maximum contractile work capacity for the unipolar PSS@CNT muscle is 0.73 J/g (Fig. 3D), which is 3.1 times that previously reported (*2*) for a CNT yarn muscle operated in an aqueous electrolyte.

Because of the high-rate capability of the unipolar PSS@CNT muscles, they can function at lower temperatures than prior-art electrochemical muscles. More specifically, a 35 wt % PSS@CNT muscle can usefully operate down to -30 °C, while providing a contractile stroke of ~2.5%, which is even higher than for the neat CNT at room or higher temperatures. A giant unipolar stroke was also obtained (Fig. 3E and F) when the 30 wt % PSS@CNT muscle was operated in an organic electrolyte, 0.2 M lithium bis(trifluoromethane)sulfonimide (LiTFSI) in dimethyl sulfoxide (DMSO). This organic electrolyte muscle provided a 2.0-fold SRES. The muscle stroke reached 17.3% for a 23.1 MPa load, and the maximum work capacity was 3.5 J/g at

0.1 Hz (Fig. 3E). The peak stroke of 18.6% for the unipolar muscle, which occurs at 0.1 Hz for a -3 to 1 V square wave, was reduced to 4.5% at 1 Hz, where the full-cycle contractile power density was 1.31 W/g (Fig. 3F). The maximum average power density was 2.9 W/g.

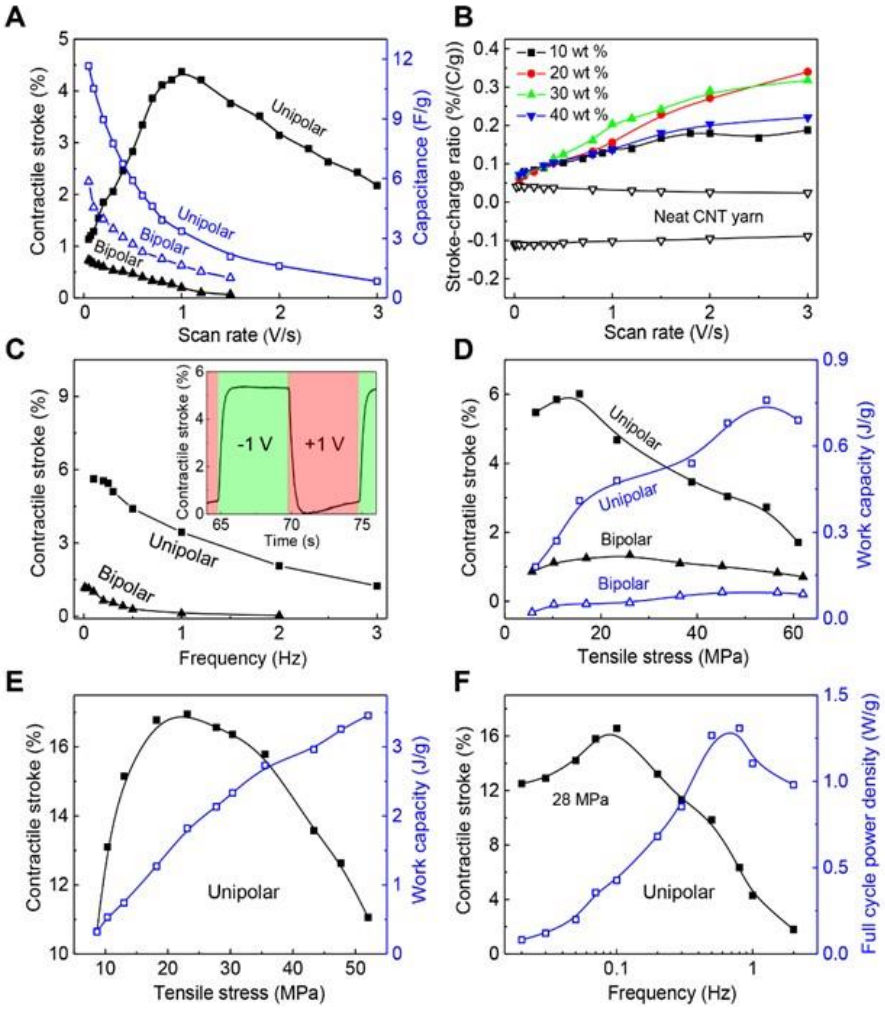

Fig. 3. Scan rate enhanced strokes for PSS@CNT unipolar muscles. (**A**) The dependence of tensile stroke and capacitance on scan rate for a unipolar PSS@CNT and a bipolar neat CNT muscle in 0.1 M aqueous LiCl. Upon increasing scan rate from 20 to 1000 mV/s, the contraction of the unipolar muscle was amplified by a factor of 3.8. (**B**) The effect of polymer content on the stroke-charge ratio for a PSS@CNT unipolar muscle. (**C**) The frequency dependence of contractile stroke on square wave pulses, which is maximized by using a voltage range between +1 V and -1 V for the above unipolar muscle, and between 0 and +1 V for the bipolar muscle. The inset shows the dependence of stroke on square wave pulses for the PSS@CNT muscle. (**D**) The dependence of equilibrium stroke and work capacity on applied tensile stress for a unipolar PSS@CNT muscle and a bipolar neat CNT muscle. (**E**) The dependence of equilibrium stroke and work capacity on tensile stress for the PSS@CNT muscle using 0.2 M LiTFSI in DMSO as electrolyte. A 0.1 Hz square wave potential change from -3 to +1 V was applied. (**F**) The dependence of contractile stroke and full-cycle power density on frequency for the muscle of (E), using the same square wave potential change and an applied tensile stress of 28 MPa.

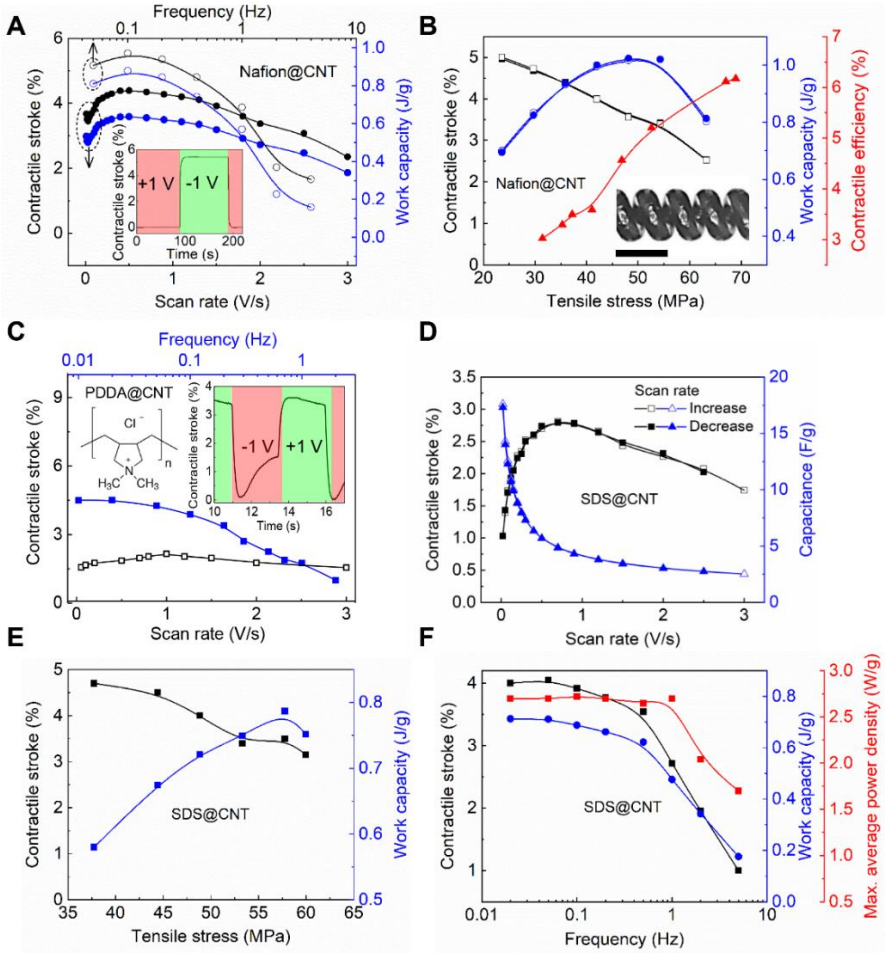

Fig. 4. Other unipolar muscles showing SRES. (**A**) For a Nafion@CNT muscle, operated in 0.2 M LiCl under 21 MPa tensile stress, the dependence of muscle stroke and work capacity on scan rate (bottom axis) and on square wave frequency (top axis) for a potential change between -1 and +1 V. The inset shows the dependence of stroke on square wave pulses for the Nafion@CNT muscle. (**B**) Contractile stroke, work capacity, and contractile efficiency versus tensile stress for the Nafion@CNT muscle. The inset shows a microscope image of the Nafion@CNT muscle (the scale bar is 150 μm). (**C**) The dependence of contractile stroke on scan rate (bottom axis) and on square wave frequency (top axis) for a PDDA@CNT muscle operated between -1 to +1 V in 0.1 M LiCl aqueous electrolyte under a 15.2 MPa stress. The inset shows the dependence of stroke on square wave pulses for the PDDA@CNT muscle. (**D-F**) For SDS@CNT and a potential range between -1 and +1 V: (D) the dependence of contractile stroke and capacitance for SDS@CNT on scan rate; (E) the dependence of contractile stroke and work capacity on the applied tensile stress; and (F) the dependence of contractile stroke, work density, and maximum average power density on square wave frequency.

The highest work capacity in an aqueous electrolyte was obtained for unipolar muscles containing Nafion. Like for 30 wt % PSS@CNT, unipolar actuation occurs for 10 wt % Nafion@CNT because of a shift of the pzc to above +1 V, which is outside the electrochemical window of the 0.2 M LiCl aqueous electrolyte. SRES also occurs for Nafion@CNT (Fig. 4A) and the peak stroke (4.3%) is similar to that for the PSS@CNT muscle (4.4%). The contractile work capacity of the Nafion@CNT reached 1.04 J/g (Fig. 4A), which is 4.4 times the previous record (*2*) for an electrochemical muscle operated in an aqueous electrolyte. The contractile efficiency (Fig. 4B) was 6.1% for a scan rate of 200 mV/s, which is even higher than the previous record (*4*)

in an organic electrolyte (5.4%). To avoid self-discharge, this maximum efficiency was obtained for a voltage range of 0.2 to -1.2 V, where the work capacity and stroke were reduced to 0.4 J/g and 2.5%, respectively. Note that a unipolar muscle cannot be made by merely inserting a Nafion membrane between muscle and counter electrodes that are operated in an aqueous LiCl electrolyte. While the inter-electrode charge transport for both electron and hole injection is exclusively by Li^+, Cl^- ions are inserted into the electrochemical double layer during hole injection. Hence, the observed actuation is bipolar and the actuation during electron injection is small, like for the bipolar neat yarn muscle (Fig. 3A).

An anion-exchange ionomer (poly (diallyldimethylammonium chloride), PDDA), shifts the pzc in the opposite direction (to below -1 V) than for cation-exchange ionomers, but unipolar strokes are still obtained. Anions are inserted or removed for PDDA@CNT, whereas cations are inserted and removed for PSS@CNT. Hence, changing the potential from +1 V to -1 V provides a -4.5% stroke for PDDA@CNT and a 5.8% stroke for PSS@CNT (Figs. 4C and 3D). Like for PSS@CNT muscles, PDDA@CNT muscles provide SRES (Fig. 4D). Unless the polymer infiltrated into the CNT yarn contains a charged functional group, the pzc is little changed and no unipolar or SRES behavior is observed. Hence, a polyvinyl alcohol (PVA) infiltrated CNT yarn operated in 0.1 M LiCl does not show SRES.

Since the PSS@CNT and PDDA@CNT yarns actuate in-phase when used as opposite electrodes, they can be mechanically coupled to provide a single muscle that utilizes the SRES enhanced strokes of both yarns to amplify the force output and eliminate the need for a passive counter electrode. By coating separated yarn pairs with a gel electrolyte (0.5 M aqueous LiCl in cellulose) to enable inter-electrode ion transport, we realized an all-solid-state PSS@CNT/PDDA@CNT muscle, whose contractile stroke in aqueous electrolyte (3.85%) is comparable to that for a PSS@CNT muscle (5.8%) and a PDDA@CNT muscle (4.5%). This elimination of the need for an electrolyte bath is important for many applications. For example, we have used these coiled PSS@CNT and PDDA@CNT muscles to make an actuating two-layer textile, in which these muscles are woven together using cotton yarn in each textile layer and these textile layers are interconnected by a PVA gel electrolyte containing 0.5 M LiCl aqueous electrolyte. The contractile stroke of this textile muscle was 3.9% in the warp direction (which is the muscle direction) for a 0.05 Hz square wave between -2 V and 2 V and an applied load of 3.4 MPa. When the square wave actuation frequency was increased to 0.5 Hz, the stroke of the actuating textile decreased to 2.7%.

Unipolar stroke muscles with SRES by surfactant absorption on coiled CNT yarns

A unipolar stroke was also observed for a coiled CNT yarn muscle in which the CNTs were coated with a surfactant, sodium dodecyl sulfate (SDS), and then cycled in a 0.2 M LiCl aqueous electrolyte containing 0.6 wt % SDS. We observed that the pzc is shifted positively to beyond the electrochemical window of this electrolyte. Together with unipolar stroke behavior, SRES was observed (Fig. 4D). A peak muscle contraction of 2.8% was obtained for a 0.9 V/s scan rate between +1 and -1 V, while the muscle contraction at a low scan rate (20 mV/s) was only 35.7% of this value, and similar to that for the neat CNT yarn in this electrolyte. The observed work capacity for square-wave excitation reached 0.79 J/g and the maximum average power density during contraction and the full cycle power density were 2.7 and 2.0 W/g, respectively (Fig. 4E and F). The contractile stroke at 1 Hz when lifting a 48 MPa load was 2.7%, and increased to a remarkable 4.0% at 0.1 Hz (Fig. 4F). High cycle life was obtained, the initial contractile stroke (3.7%) decreased by only 6.2% during the first 8000 cycles. If there was 0.6 wt % SDS in the electrolyte and no SDS was initially coated on the yarn, the stroke was initially bipolar and then

fully converted to unipolar after ~5000 cycles, as a result of SDS absorption on the CNT yarn. was initially bipolar and then fully converted to unipolar after ~5000 cycles, as a result of SDS absorption on the CNT yarn. This absorption during 22 hours of electrochemical cycling provided a contractile stroke of 3.5% for a potential rate of 1 V/s between +1 and -1 V.

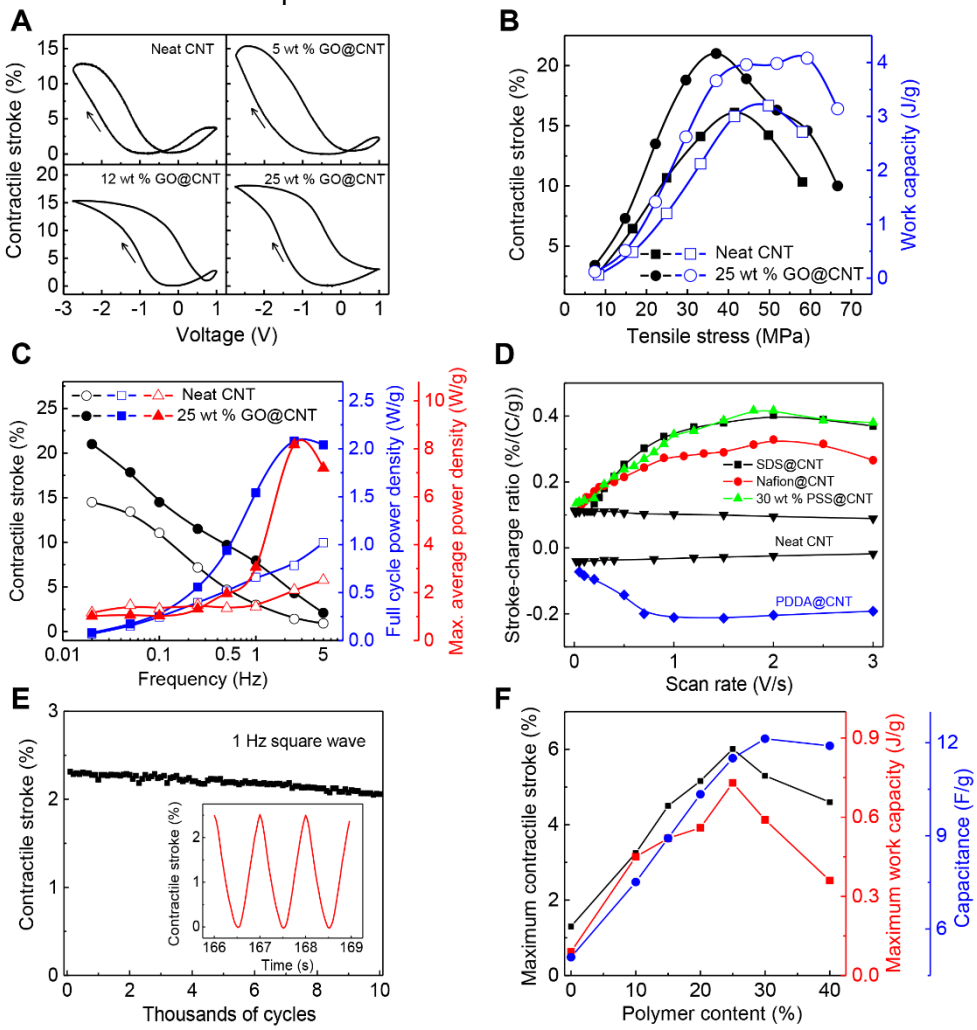

Fig. 5. (**A**) Contractile stroke during CV scans at 25 mV/s for neat CNT yarn and for GO@CNT yarns containing differing amounts of GO, which are actuated in 0.2 M TBA·PF_6 in acetonitrile. (**B**) Contractile stroke and work capacity versus applied tensile stress for neat CNT yarn and 25 wt % GO@CNT yarn, when actuated at a square wave frequency of 0.02 Hz and a potential change from -2.75 to +1 V. (**C**) Contractile stroke, full cycle power density, and maximum average power density versus square wave frequency for actuation of a neat CNT yarn and a 25 wt % GO@CNT using the above electrolyte and potential range. (**D**) Stroke-charge ratio versus potential scan rate for unipolar muscles having SRES and a bipolar neat CNT muscle that does not have SRES. The electrolyte used was 0.1 M LiCl for PSS@CNT, PDDA@CNT, and the neat CNT yarn; 0.2 M LiCl for Nafion@CNT and SDS@CNT. (**E**) Contractile stroke versus cycle number for the 30 wt % PSS@CNT unipolar muscle. The inset shows the time dependence of square wave contractile stroke during cycling. (**F**) The load optimized maximum contractile stroke and work capacity and the capacitance per CNT weight at fixed load (10.8 MPa) for PSS@CNT yarns containing different weight percentages of PSS polymer when actuated in 0.1 M LiCl.

Using this approach for a sheath-run artificial muscle (SRAM), we obtained a usable muscle stroke (1.3%) at a remarkably high frequency (10 Hz) when operating in a 0.2 M LiCl aqueous

electrolyte containing 0.6 wt % SDS. This outstanding high frequency capability results from the combination of SRES behavior and the short diffusion distance for actuating the sheath, compared with the diffusion distance for actuating a CNT yarn that has the same mass of CNTs per muscle length. The precursor CNT@nylon6 SRAM was made by a process we previously described (*5*), except that SDS was coated on the CNTs in the sheath after low twist was inserted.

Unipolar muscles without SRES by biscrolling graphene oxide

We also made unipolar muscles by biscrolling graphene oxide (GO) into a CNT yarn. During biscrolling, a guest-coated CNT sheet stack is twist inserted, so that the guest is trapped inside the helical corridors of the yarn (*6*). An organic electrolyte (0.2 M TBA·PF_6 in acetonitrile, where TBA is tetrabutylammonium) was used. With increasing GO content, the stroke of a CNT yarn muscle gradually changed from bipolar to unipolar (Fig. 5A). The peak equilibrium tensile contraction and work capacity were 21% and 4.1 J/g, respectively, compared with 16% and 3.2 J/g for the neat yarn in this electrolyte (Fig. 5B). This muscle retains 80% of its stroke after 10 thousand cycles. Due to the substantial absence of charge-containing functional groups, reducing the 50 wt % GO@CNT yarn resulted in a rGO@CNT yarn muscle that provided little pzc shift for both aqueous and non-aqueous electrolytes, so bipolar actuation was obtained.

The contractile stroke of the unipolar GO@CNT muscle at 1 Hz was 8.0% (Fig. 5C), compared to 2.5% for the neat CNT muscle and the previous 4.7% for a sheath-run CNT muscle (*5*) at this frequency. Also important, the full-cycle contractile power and the maximum average power during contraction were 2.08 and 8.17 W/g, respectively, for the GO@CNT muscle, compared with 1.02 and 2.52 W/g, respectively, for a neat CNT yarn muscle (Fig. 5C). For further comparison, the highest previously reported full-cycle contractile power and maximum contractile average power for operation in an organic electrolyte were 0.99 and 3.71 W/g for a sheath-run artificial muscle. Instead of using GO as a yarn guest, oxidizing the surface of CNTs in a yarn, using boiling nitric acid, also results in unipolar behavior (with the stroke twice that of the neat bipolar CNT yarn), but SRES was absent.

Unipolar stroke without SRES for neat CNT yarns in a single-mobile-ion aqueous electrolyte

A unipolar stroke is both expected and observed for electrolytes in which only ions of one sign are mobile. We observed this behavior for a neat CNT yarn muscle that is electrochemically driven in an aqueous electrolyte (5 mg/mL of PSS in water), in which the only mobile ion is Na^+. Also, depending upon the potential scan rate, either bipolar or unipolar actuation was obtained for a neat CNT yarn in an electrolyte having two mobile ions (0.1 M aqueous LiCl electrolyte). For all scan rates, the compensation of electrons injection is by injection of Li^+ into the double layer. However, for high scan rates, the lower mobility of Cl^- means that hole injection is increasingly compensated by the removal of Li^+ from the double layer. Hence, unipolar behavior is observed for a scan rate of 2 V/s. No SRES was observed, so the obtained muscle stroke was low for all scan rates. This type of unipolar stroke behavior, without SRES, is well known for Faradaic conducting polymer artificial muscles.

Theoretical and experimental analysis of unipolar behavior and SRES

Previous results for step-containing Pt surfaces have suggested that the change in pzc should be linearly correlated with the change in work function (*7*). The effect of charged groups on shifting the work function was calculated using density functional theory (DFT), using graphene as the model conductor, and compared with experimental results on the effects of these groups for shifting the pzc of ionomer-containing CNT muscles (PSS@CNT and PDDA@CNT). Exceptional agreement was obtained between the observed dependence of pzc on the ratio of SO_3^- groups and

electrochemically accessible surface carbon atoms, and the theoretically calculated dependence of work function on this ratio. Additionally, the effect of positively charged ammonium groups in PDDA was calculated and found to provide an identical shift for the same ratio of ionic groups to electrochemically accessible surface carbon atoms. Moreover, presented theoretical results predict that structures containing mixtures of non-infiltrated and ionomer-infiltrated yarns should have a pzc that is the average of the component structures. We have demonstrated this averaging for coiled yarns and plied coiled yarns having neat CNT yarns and PSS infiltrated yarns in different electrically contacting yarn lengths.

The existence of SRES implies that there is a scan rate dependence of the effective ion size. This effective ion size is the sum of the ion size due to ion solvation and the solvent that is dragged into the yarn by the moving solvated ions. Hence, the remarkable performance of our SRES muscles results from electroosmotic pumping, as well as the wide potential window enabled by unipolar behavior. The transport of free solvent is well known for a host of electrochemical devices, including ion pumps for transporting fluids, ionic polymer-metal composites (IPMCs) cantilever actuators, and fuel cells. If little or no ion solvation can occur, SRES cannot result. We demonstrated this by observing the absence of SRES for actuation of PSS@CNT in an ionic liquid and in water-in-salt electrolytes, where little water is available for solvation (*8*).

In order to quantify the effects of SRES on effective ion volume, the scan-rate dependence of the stroke-charge ratio (SCR) was obtained for the presently investigated SRES muscles. For this comparative work, the same potential range was used for all unipolar muscles, and potential ranges were chosen for bipolar muscles in order to avoid stroke cancellation. These results for the aqueous LiCl electrolyte (Fig. 5D) show that the SCR is small and even slightly decreases with increasing potential scan rate for the neat CNT yarn, similarly enhanced for PSS@CNT and SDS@CNT, and less enhanced for Nafion@CNT.

For very high scan rates, the SCR becomes less dependent on scan rate and eventually decreases. This saturation of SCR for very high scan rates contrasts with the linear dependence on current amplitude that is observed for the electroosmotic transport of water through a membrane (*9*). The explanation for this saturation is that the current for high potential scan rates varies over a wide range, so the SCR for high potential scan rates will not be the same as the SCR for galvanostatic scans. This conclusion is supported by our measurements of SCR for galvanostatic charging (i.e., constant current density charging) of a 36 wt % PSS@CNT muscle and a SDS@CNT muscle, which shows that the SCR approximately linearly depends upon the applied current density. Like for the constant potential scan rate SCR, the low current density SCR is about 0.1 %/(C/g). However, the galvanostatic SCR increases with increasing current density to 0.66 %/(C/g), compared with a maximum of 0.42 %/(C/g) for the constant-scan-rate SCR.

The above processes partially explain why muscle strokes are additive for galvanostatic stroke changes for different potential ranges, while they are not additive for fast constant-scan-rate actuation and for square wave actuation. Also, the sum of the charge injected at high potential scan rates for a potential scan from V_1 to V_3 is larger than the sum for a potential scan from V_1 to V_2 and from V_2 to V_3, where $V_3 > V_2 > V_1$. Likewise, for high frequency square wave actuation, the charge injected for a potential change between V_1 and V_3 is larger than the sum of the charge injected for potential changes between V_1 and V_2 and between V_2 and V_3. This aspect has not previously been described, since previous electrochemical muscles had such a low stroke for fast actuation that it could not be investigated.

The capacitance (per CNT weight) of the PSS@CNT muscle dramatically increases with increasing content of PSS, which increases muscle stroke (Fig. 5F). Also, the concentration

dependence of capacitance of the full coiled PSS@CNT muscle is close to that for the precursor PSS@CNT sheet stack. The most reasonable explanation is that the PSS effectively freezes inter-nanotube interactions in the CNT sheets and twisted yarns, with respect to twist-induced decreases in capacitance.

Even though actuation carries a non-equilibrium content of solvent into the muscle, because of electroosmotic drag, muscle stroke is largely retained over a thousand seconds, even when the power source is disconnected. However, small relaxation of muscle stroke occurs within a few seconds for 5 mHz square wave actuation of a PSS@CNT muscle, which depends upon the cycling history. Such phenomena are observed for all investigated SRES muscles, and is most likely explained by partial loss of dragged solvent. Upon increasing the actuation frequency, this back relaxation disappears because of switching to a new actuation cycle.

Summary

This work demonstrates new concepts for electrochemically powered yarn muscles, which provide higher performance in terms of stroke, work capacity, power density, and efficiency than previously known electrochemical muscles. This first newly applied and theoretically analyzed concept for a yarn muscle is to use pzc shift agents (include ion-exchange membrane polymers, oxidized graphene platelets, and ionic surfactants) to shift the pzc to outside the potential window of the electrolyte, thereby eliminating the destructive effects of bipolar behavior. The second concept is to demonstrate that selected unipolar muscles can provide dramatically enhanced performance because of electroosmotic pumping of solvent to within muscles, so that muscle stroke dramatically increases with increasing potential scan rate. This SRES phenomenon enables the normal decay of muscle stroke with decreasing charge injection on increasing potential scan rate to be overcome by electroosmotic pumping that increases the effective ion size that drives actuation. The maximum strokes obtained at 1 Hz using prior-art technologies were 4.7% and 1.1% for organic electrolyte and aqueous electrolyte, respectively, compared to the presently demonstrated maximum strokes of 8.0% and 3.9% at this frequency for unipolar muscles. The highest previously reported work capacities and maximum average power densities for electrochemical muscles were 3.8 J/g (*10*) and 3.17 W/g (*5*) for an organic electrolyte, and were 0.236 J/g and 0.02 W/g for an aqueous electrolyte (*2*). Our new high-cycle-life muscles have increased these metrics to 4.08 J/g and 8.17 W/g for an organic electrolyte, and 1.04 J/g and 2.70 W/g for an aqueous electrolyte. The advantages of these unipolar muscles having SRES are demonstrated for all-solid-state muscles and muscle textiles that eliminate the need for an electrolyte bath.

2. Project Supported Archival Publications During the Third Project Year

1. “Electrical energy harvesting from ferritin biscrolled carbon nanotube yarn”, H. Kim, J. W. Park, J. S. Hyeon, H. J. Sim, Y. Jang, Y. Shim, C. Huynh, R. H. Baughman, S, J. Kim, *Biosensors and Bioelectronics* **164**, 112318 (2020).

2. “Self-powered carbon nanotube yarn for accelerometer sensor application", B. J. Kim, Y. Jang, J. H. Moon, R. H. Baughman, S. J. Kim, *IEEE Transactions on Industrial Electronics* **68**, 2676-2683 (2021).

3. "Humidity and water-responsive torsional and contractile lotus fiber yarn artificial muscles", Y. Wang, Z. Wang, Z. Lu, M. Jung de Andrade, S. Fang, Shaoli Z. Zhang, J. Wu, R. H. Baughman, *ACS Appl. Mater. Interfaces* **13**, 6642-6649 (2021).

4. “Unipolar-stroke, electroosmotic-pump carbon nanotube yarn muscles”, H. Chu, X. Hu, Z. Wang, J. Mu, N. Li, X. Zhou, S. Fang, C. S. Haines, J. W. Park, S. Qin, N. Yuan, J. Xu, S. Tawfick, H. Kim, P. Conlin, M. Cho, K. Cho, J. Oh, S. Nielsen, K. A. Alberto, J. M. Razal, J. Foroughi, G. M. Spinks, S. J. Kim, J. Ding, J. Leng, R. H. Baughman, *Science* **371**, 494-498 (2021).

3. US Patent Issuances During the Project Year on Work That Has Been AFOSR-Supported

1. “Incandescent tension annealing processes for strong, twist-stable carbon nanotube yarns and muscles”, US 10,837,130 (Issued 11/17/2020).

2. “Coiled and twisted nanofiber yarns for electrochemically harvesting electrical energy from mechanical deformation”, US 11,085,422 (Issued 8/10/2021).

4. US Patent Allowances During the Project Year on Work That Has Been AFOSR-Supported

1. “Actuating textiles containing polymer fiber muscles”, 16/087,540 (PCT/US2017/023438), accepted by US Patent Office on or before 3/26/2021).

2. “Coiled, twisted nanofiber yarn and polymer fiber torsional actuators”, 16/596,921, accepted by US Patent Office on or before 6/4/2021.

3. “Thermally-powered coiled polymer fiber tensile actuator system and method”, 16/685,904, accepted by US Patent Office 6/18/2021.

5. US Patent Filings During the Project Year on Work That Has Been AFOSR-Supported

1. “Methods or torsional refrigeration by twisted, coiled, and supercoiled fibers and systems thereof”, Appl. No. 17/036, 018, filed 9/29/2020.

2. “Actuating textiles containing polymer fiber muscles”, US 2021/0198817 A1 (pub. date: 7/1/2021).

REFERENCES

1. H. Chu et al., Unipolar stroke, electroosmotic pump carbon nanotube yarn muscles, *Science* **371**, 494–498 (2021).
2. J. Qiao et al., Large-stroke electrochemical carbon nanotube/graphene hybrid yarn muscles, *Small* 1801883 (2018).
3. S. H. Kim et al., Harvesting electrical energy from carbon nanotube yarn twist, *Science* **357**, 773-778 (2017).
4. J. A. Lee et al., Electrochemically powered, energy-conserving carbon nanotube artificial muscles, *Advanced Materials* **27**, 1700870 (2017).
5. J. Mu et al., Sheath-run artificial muscles, *Science* **365**, 150–155 (2019).
6. M. D. Lima et al., Biscrolling nanotube sheets and functional guests into yarns, *Science* **331**, 51-55 (2011).
7. S. Trasatti, Work function, electronegativity, and electrochemical behaviour of metals: II. Potentials of zero charge and “electrochemical” work functions. *Journal of Electroanalytical Chemistry and Interfacial Electrochemistry* **33**, 351-378 (1971).

8. L. Suo et al., Water-in-salt electrolyte enables high-voltage aqueous lithium-ion chemistries, *Science* **350**, 938-943 (2015).
9. X. Ren et al., Electro-osmotic drag of water in ionomeric membranes: new measurements employing a direct methanol fuel cell, *J. Electrochem. Soc.* **144**, 267-270 (1997).
10. K. J. Kim et al., Enhancing the work capacity of electrochemical artificial muscles by coiling plies of twist-released carbon nanotube yarns, *ACS Applied Materials & Interfaces* **11**, 13533-13537 (2019).